

BER analysis of FBMC-OQAM systems with Phase Estimation Error

Rafik Zayani^{1,*}, Hmaied Shaiek², Daniel Roviras², Yahia Medjahdi²

¹Innov'Com, Sup'Com, Carthage University, Tunis, Tunisia

²CEDRIC/LAETITIA, CNAM, Paris, France

*rafik.zayani@supcom.tn

Abstract: This paper analyzes the bit-error-rate (BER) performance of filter bank multicarrier systems with offset quadrature amplitude modulation (FBMC-OQAM) in the presence of phase offset. We consider that the FBMC intrinsic-interference has a Gaussian probability distribution, and we derive the BER analytical expressions for multilevel modulation (M-OQAM) over Rayleigh flat fading channels. Analytical expressions developed in this paper are checked and confirmed by computer simulations.

1. Introduction

In each generation of cellular wireless networks, the physical layer technology has always served as a cornerstone and must be judiciously chosen. As a recent example, in the fourth generation (4G) Long Term Evolution (LTE) and LTE-Advanced, cyclically prefixed orthogonal frequency division multiplexing (CP-OFDM) has been adopted [1]. CP-OFDM offers many attractive advantages such as efficient hardware implementation, low complexity equalization, compatibility with multiple-input multi-output (MIMO) technologies. However, CP-OFDM suffers from high spectral side lobes resulting from the Sinc pulse shape in the frequency domain. This can lead to many issues, such as the significant loss of spectrum efficiency, 10 percent of the system bandwidth was reserved as guard band in LTE [2], and the stringent synchronization requirement. Indeed, to achieve intercarrier-interference (ICI) free, the uplink users' signals must be synchronized at the receiver input. Any timing misalignment larger than the CP would lead to large performance degradation. Therefore, additional signal-processing solutions have to be considered to maintain the orthogonality in the reception.

On the other hand, fundamental research towards future (5G) networks is ongoing and driven by the next foreseen emerging services [2]: enhanced mobile broadband (eMBB), massive machine-type communication (mMTC), and ultra-reliable and low-latency communication (URLLC), where data rates are expected to increase 1000 times, and the number of connected devices will be 10-100 times higher than today. These services impose new challenges due to the massive wireless connectivity between machines. One of these challenges is the sporadic access requiring relaxed synchronization schemes and access to fragmented spectrum to limit the signaling overhead [3]. It is unlikely that challenges can be satisfied using Orthogonal Frequency Division Multiplexing (OFDM) adopted by the current LTE-A due to its strong out-of-band (OOB) radiation and suboptimal spectrum shape.

To overcome the shortcomings of the classical OFDM, filter-bank multicarrier with offset quadra-

ture amplitude modulation (FBMC-OQAM) has been introduced [4] for the next generation (5G) of wireless networks. FBMC-OQAM employs well-localized band-limited pulse shaping filters that overlap in time [5][6][7]. In FBMC-OQAM, an orthogonal condition of filter is satisfied only in a real domain. Therefore, each subcarrier is modulated in OQAM where the real and imaginary values are time staggered by the half of the symbol duration [8][1]. The purpose of OQAM is to ensure that the real and imaginary elements on the time-frequency lattice are staggered so as to dodge the intrinsic interference [9]. Indeed, FBMC-OQAM data is real, and an imaginary intrinsic-interference occurs in the transmission process. This interference, caused by the data symbols transmitted in the neighborhood area in the time-frequency domain, is orthogonal to the useful data symbols. Then, the detection process is easily performed when the channel is flat fading or slowly selective [9]. Nevertheless, a phase shift in the detection process of the user of interest data symbols can be very harmful to the performance of FBMC-OQAM [12], although its robustness to the asynchronism, timing offset (TO) or carrier frequency offset (CFO), caused by other users. Then, in this paper, we are interested in the phase shift occurred in the chain of the user of interest.

In [10], authors have investigated the bit error rate performance of FBMC-OQAM in the presence of phase error using the discrete probability distribution of the intrinsic-interference. This investigation was limited to 4-OQAM constellation and AWGN channel. More recently, Rostom et al. [9] have introduced symbol error rate (SER) expressions, by approximating the intrinsic-interference probability density as Gaussian one, for any 2^m -PAM data mapping and a constant phase error but only for AWGN channel. Since the intrinsic-interference is independent to the Gaussian noise, it contributes as a part of the noise and the SER derivation is a simple extension from the classical SER expression. However, in a random channel case, the intrinsic-interference depends on the channel gain that makes the SER derivation very complicated. Indeed, we have to evaluate an intractable integration where the Rayleigh gain appears both in the numerator (signal part) and in the denominator (interference part) of the integrand. It is worth mentioning that in [25] authors have investigated the differences between the performances of 4-QAM and 4-OQAM in the presence of carrier-synchronization phase ambiguity but in case of single carrier modulations. To the best of authors' knowledge, there is no explicit BER expression is given for multilevel M-OQAM based FBMC with phase offset in Rayleigh channel. In this paper, we provide a general analysis for the impact of phase offset on the BER performance of M-OQAM based FBMC over Rayleigh flat fading channels. In particular, we derive the exact BER of M-OQAM by considering the Gaussian intrinsic-interference approximation. These BER expressions can be evaluated without any numerical integration method.

The remainder of this paper is organized as follows: Section II is dedicated to present the considered FBMC-OQAM system. In section III, we derive the exact expressions of the BER performance of M-OQAM based FBMC in the presence of phase estimation error. Numerical results are provided in section IV, followed by the conclusion in section V.

Notations : $(\cdot)^*$ denotes the complex conjugate operation and $\langle \cdot, \cdot \rangle$ stands for the inner product.

2. The FBMC-OQAM System

We consider FBMC system with N subcarriers that are modulated by data symbols taken from M-OQAM constellation. The baseband discrete-time model of a typical FBMC-OQAM modulated

signal is given by [11]

$$s[m] = \sum_{p=0}^{N-1} \sum_{q=-\infty}^{+\infty} a_{p,q} \underbrace{g[m - qN/2] e^{j\frac{2\pi}{N}p(m-\frac{D}{2})} e^{j\varphi_{p,q}}}_{\gamma_{p,q}[m]} \quad (1)$$

where $a_{p,q}$ are real-valued symbols, which are the real or the imaginary parts of QAM symbols, $g[m]$ is the prototype filter impulse response taking values in real field and $\gamma_{p,q}[m]$ are the shifted versions of $g[m]$ in time and frequency. The phase term $\varphi_{p,q}$ is given by $\varphi_{p,q} = \frac{\pi}{2}(p+q) - \pi pq$ and the delay term $\frac{D}{2}$ depends on the length (L) of $g[m]$. We have $D = KN - 1$ and $L = KN$, where K is the overlapping factor.

In a distortion-free noiseless channel, the demodulated signal r_{p_0,q_0} at time instant q_0 and sub-carrier p_0 is given by

$$r_{p_0,q_0} = \langle s, \gamma_{p_0,q_0}^* \rangle = \sum_{m=-\infty}^{m=+\infty} s[m] \gamma_{p_0,q_0}^*[m]$$

$$f = a_{p_0,q_0} + \underbrace{\sum_{p \neq p_0} \sum_{q \neq q_0} a_{p,q} \sum_{m=-\infty}^{+\infty} \gamma_{p,q}[m] \gamma_{p_0,q_0}^*[m]}_{j u_{p_0,q_0}} \quad (2)$$

2.1. Intrinsic-interference Distribution

According to [11], the prototype filter is designed such that the intrinsic-interference term is orthogonal to the useful symbol i.e. $j u_{p_0,q_0}$ is pure imaginary-valued.

Let's simplify $\sum_{m=-\infty}^{+\infty} \gamma_{p,q}[m] \gamma_{p_0,q_0}^*[m]$ as $\chi_{\Delta p, \Delta q}$, which are the transmultiplexer impulse response coefficients. $\chi_{\Delta p, \Delta q}$ can be calculated assuming null data except the considered symbol (p_0, q_0) where a unit impulse is applied [9].

Then $\chi_{\Delta p, \Delta q}$ can be derived as in [9]

$$\chi_{\Delta p, \Delta q} = \sum_{m=-\infty}^{+\infty} g[m] g[m - \Delta q N/2] \times e^{j\frac{2\pi}{N} \Delta p (\frac{D}{2} - m)} e^{j\pi (\Delta p + p_0) \Delta q} e^{-j\frac{\pi}{2} (\Delta p + \Delta q)} \quad (3)$$

where $\Delta p = p_0 - p$ and $\Delta q = q_0 - q$. Since the most part of the energy of the impulse response is localized in a restricted set around the considered symbol (denoted by Ω_{p_0,q_0}), the intrinsic-interference $j u_{p_0,q_0}$ can be expressed as

$$j u_{p_0,q_0} = \sum_{(p,q) \in \Omega_{p_0,q_0}} a_{p,q} \chi_{\Delta p, \Delta q} \quad (4)$$

The coefficients $j u_{p_0,q_0}$ represent the sum of many independent and identically distributed random variables. They are depicted by Table 1 where the PHYDYAS prototype filter [4] with overlapping factor set to $K = 4$ is considered.

Here, we note that the resulting interference term is a sum of at least twenty independent random variables where the distribution of each of these variables depends on the modulation order.

This article has been accepted for publication in a future issue of this journal, but has not been fully edited. Content may change prior to final publication in an issue of the journal. To cite the paper please use the doi provided on the Digital Library page.

Table 1. Transmultiplexer impulse response

	$q_0 - 3$	$q_0 - 2$	$q_0 - 1$	q_0	$q_0 + 1$	$q_0 + 2$	$q_0 + 3$
$p_0 - 1$	$0.043j$	$-0.125j$	$0.206j$	$0.239j$	$-0.206j$	$-0.125j$	$-0.043j$
p_0	$-0.067j$	0	$0.564j$	0	$0.564j$	0	$-0.067j$
$p_0 + 1$	$-0.043j$	$-0.125j$	$-0.206j$	$0.239j$	$0.206j$	$-0.125j$	$0.043j$

Based on the central limit theorem, the probability distribution of the intrinsic-interference can be approximated by a zero-mean Gaussian random variable with a variance $\sigma_u^2 = (\log_2(M)^2 - 1)/3$.

In figures (1) and (2), the exact probability distribution of the intrinsic-interference is compared to the Gaussian one for modulation orders $M = 16$ and $M = 64$, respectively.

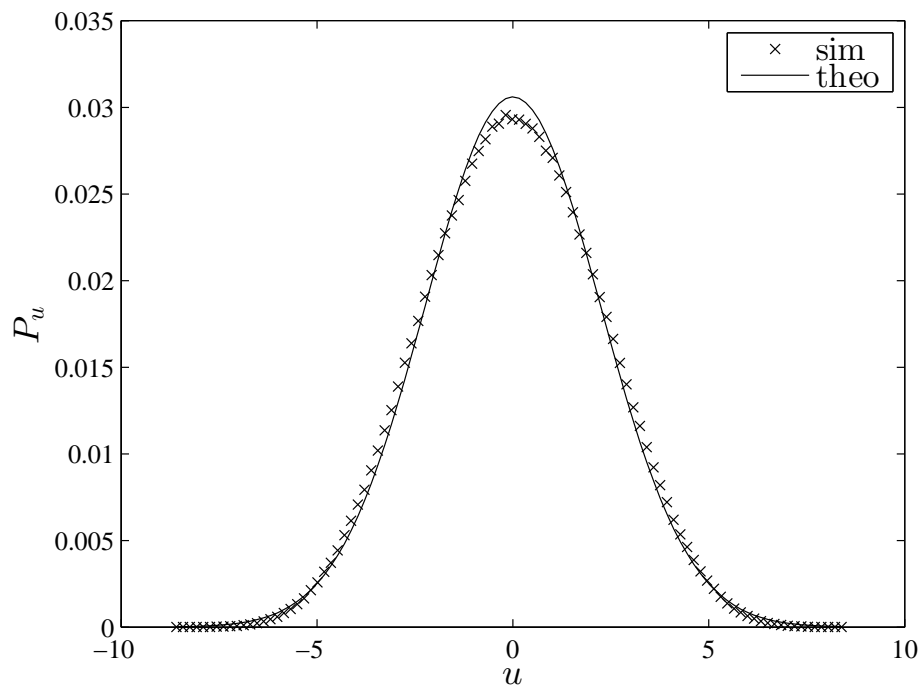


Fig. 1. Probability distribution comparison: Simulation vs. Theoretical approximation for 16-QAM

We can see that the theoretical approximation shows a good match to the corresponding simulation probability distribution. Moreover, in order to measure how well the proposed approximation matches the exact distribution, we use the well-known Kullback-Leibler distance (D_{KL}) that is given by equation (5).

$$D_{KL}(P_u, Q) = \sum_{u \in U} P_u(u) \log \frac{P_u(u)}{Q(u)} \quad (5)$$

where P_u is the exact intrinsic-interference probability distribution and Q is theoretical approx-

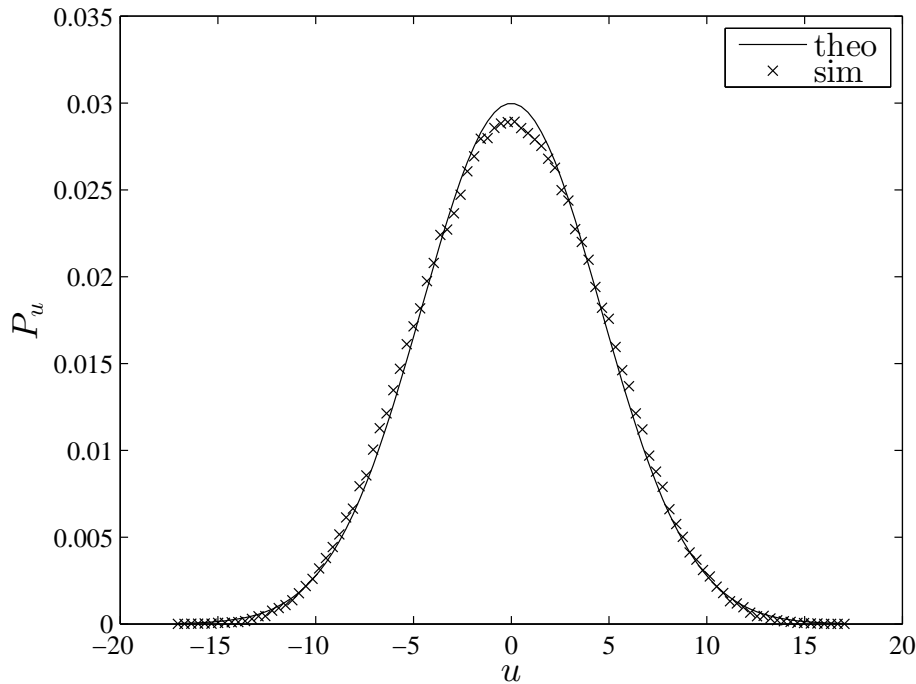


Fig. 2. Probability distribution comparison: Simulation vs. Theoretical approximation for 64-QAM

imation, which is considered as the Gaussian and expressed as $\frac{1}{\sqrt{2\pi\sigma_u^2}} \int_{\mathbb{R}} e^{-\frac{u^2}{2\sigma_u^2}}$.

The obtained Kullback-Leibler distances for 16-QAM and 64-QAM are about 2×10^{-3} .

2.2. FBMC-OQAM receiver

The received signal r_{p_0, q_0} is simplified as

$$r_{p_0, q_0} = a_{p_0, q_0} + ju_{p_0, q_0} \quad (6)$$

When FBMC signal passes through the channel, the channel coefficients are considered as constant during the restricted set Ω_{p_0, q_0} , and received signal can be written as

$$r_{p_0, q_0} = h_{p_0, q_0}(a_{p_0, q_0} + ju_{p_0, q_0}) + w_{p_0, q_0} \quad (7)$$

where $h_{p_0, q_0} = \alpha e^{j\theta}$ is the complex channel coefficient and w_{p_0, q_0} is the gaussian noise term with variance $\sigma_w^2 = (N_0/2)$.

3. BER Performance Analysis

Fundamental detection process of FBMC signal can be described as in equation (8). Here for concise expressions and without loss of generality, the subscript of subcarrier and time index are

removed. When linear equalizer is used, for example zero-forcing (ZF) in this paper, real-valued OQAM symbols are recovered as follows

$$r_d = \Re \left\{ \frac{r}{\hat{h}} \right\} \quad (8)$$

where $\hat{h} = \hat{\alpha}e^{j\hat{\theta}}$ is the channel estimate and $\Re\{\cdot\}$ means taking the real part.

In order to estimate \hat{h} , several channel estimation techniques for preamble-based FBMC systems have been introduced in the literature [13]-[20]. Among all these techniques, the interference approximation method (IAM), which is capable of computing an approximation of the interference from neighboring symbols [21][22], is the widely studied [14]-[16]. Interested reader can refer to [23], where challenges and solutions in channel estimation for preamble- and pilot-aided methods based FBMC systems are studied and reported.

In this paper, we analyze the impact of a channel estimation error on the performances of FBMC systems. We are, in particular, interested in an estimation error of the phase and not of the amplitude because this latter represents the same contribution as in the classical OFDM.

Given the phase estimate error $\psi = \theta - \hat{\theta}$ and assuming a perfect amplitude estimation $\hat{\alpha} = \alpha$, real-valued symbol and intrinsic-interference could interfere and the input of the decision device is then

$$r_d = (a\cos(\psi) - u\sin(\psi)) + \Re \left\{ \frac{w}{\hat{h}} \right\} \quad (9)$$

We assume a slow-varying Rayleigh flat-fading channel, where the amplitude α follows the Rayleigh probability density function with an average fading power $\nu = \mathbb{E}[\alpha]$.

3.0.1. Conditional BER: Consider first 16-OQAM. For each bit stream, we calculate the conditional BER bit by bit for the signal components, where $a \in \{-3, -1, 1, 3\}$. Since the transmitted symbols are affected by an interference term u , the distance from a received bit point to the separation axes obviously depends on the interference value u , the rotation phase ψ and the Rayleigh gain α . Take the MSB as an example: a bit error occurs when the signal representing bit 0, i.e., $a = 3, 1$, falls into the decision boundaries of bit 1, and vice versa. Therefore, the bit-error probability of the MSB conditioned on α , u and ψ is given by equation (10).

$$P_1(\alpha, u, \psi) = \frac{1}{2}Q \left(\frac{[3\cos(\psi) - u\sin(\psi)]\alpha}{\sigma_w} \right) + \frac{1}{2}Q \left(\frac{[\cos(\psi) - u\sin(\psi)]\alpha}{\sigma_w} \right) \quad (10)$$

Similarly, the conditional BER of the LSB is given by equation (11).

$$P_2(\alpha, u, \psi) = \frac{1}{2} \left[Q \left(\frac{[3\cos(\psi) - u\sin(\psi) - 2]\alpha}{\sigma_w} \right) - Q \left(\frac{[3\cos(\psi) - u\sin(\psi) + 2]\alpha}{\sigma_w} \right) \right] + \frac{1}{2} \left[Q \left(\frac{[-\cos(\psi) + u\sin(\psi) + 2]\alpha}{\sigma_w} \right) + Q \left(\frac{[\cos(\psi) - u\sin(\psi) + 2]\alpha}{\sigma_w} \right) \right] \quad (11)$$

Given that each bit is mapped to the MSB or the LSB with equal probability, the BER condi-

tioned on α , u and ψ for 16-OQAM is given by equation (12).

$$\begin{aligned}
 BER_{16OQAM}(\alpha, u, \psi) &= \frac{1}{2} [P_1(\alpha, u, \psi) + P_2(\alpha, u, \psi)] \\
 &= \frac{1}{4} \left[Q \left(\frac{[3\cos(\psi) - u\sin(\psi)]\alpha}{\sigma_w} \right) + Q \left(\frac{[\cos(\psi) - u\sin(\psi)]\alpha}{\sigma_w} \right) + Q \left(\frac{[3\cos(\psi) - u\sin(\psi) - 2]\alpha}{\sigma_w} \right) \right] \\
 &\quad + \frac{1}{4} \left[-Q \left(\frac{[3\cos(\psi) - u\sin(\psi) + 2]\alpha}{\sigma_w} \right) + Q \left(\frac{[-\cos(\psi) + u\sin(\psi) + 2]\alpha}{\sigma_w} \right) + Q \left(\frac{[\cos(\psi) - u\sin(\psi) + 2]\alpha}{\sigma_w} \right) \right] \quad (12)
 \end{aligned}$$

The BER expression in equation (12) can be simplified as

$$BER_{16OQAM}(\alpha, u, \psi) = \sum_{i=1}^6 w_i Q \left(\frac{[a_i \cos(\psi) - \ddot{a}_i u \sin(\psi) + b_i] \alpha}{\sigma_w} \right) \quad (13)$$

where the coefficients w_i , a_i and b_i are listed in Table 2 and \ddot{a}_i means the sign of a_i .

Table 2 Coefficients in the BER of 16-QAM [24]

i	$w_i =$	$a_i =$	$b_i =$
	$\frac{1}{4} \times$	$\frac{1}{\sqrt{5}} \times$	$\frac{1}{\sqrt{5}} \times$
1	1	3	0
2	1	1	0
3	1	3	-2
4	-1	3	2
5	1	-1	2
6	1	1	2

3.0.2. Average BER: The final BER of 16-OQAM is obtained by averaging the conditional BER in (13) over the Rayleigh amplitude distribution and then the intrinsic-interference distribution as shown in (14).

$$\begin{aligned}
 BER_{16OQAM}^{rayleigh}(\psi) &= \\
 &\frac{1}{4} \sum_{i=1}^6 w_i \int_{\mathbb{R}} \frac{e^{-\frac{u^2}{2\sigma_u^2}}}{\sqrt{2\pi\sigma_u^2}} \int_0^\infty \frac{\alpha}{\nu} e^{-\frac{\alpha^2}{2\nu}} Q \left(\frac{[a_i \cos(\psi) - \ddot{a}_i u \sin(\psi) + b_i] \alpha}{\sigma_w} \right) d\alpha du \quad (14)
 \end{aligned}$$

Defining

$$\mathcal{J}(u, \psi, a_i, b_i) = \int_0^\infty \frac{\alpha}{\nu} e^{-\frac{\alpha^2}{2\nu}} \times Q \left(\frac{[a_i \cos(\psi) - \ddot{a}_i u \sin(\psi) + b_i] \alpha}{\sigma_w} \right) d\alpha \quad (15)$$

Since α is Rayleigh distributed, α^2 has a chi-squared distribution with a probability density function $p(\alpha^2) = \frac{1}{\gamma} e^{-\frac{\alpha^2}{\gamma}}$ and $\gamma = \mathbb{E}[\alpha^2]$.

Then, \mathcal{J} can be written as

$$\mathcal{J}(u, \psi, a_i, b_i) = \int_0^\infty \frac{1}{\gamma} e^{-\frac{\alpha}{\gamma}} \times Q \left(\sqrt{\frac{[a_i \cos(\psi) - \ddot{a}_i u \sin(\psi) + b_i]^2 \alpha^2}{\sigma_w^2}} \right) d\alpha \quad (16)$$

and using integration by parts, it can be shown that

$$\mathcal{J}(u, \psi, a_i, b_i) = \frac{1}{2} \left[1 - \frac{a_i \cos(\psi) - \ddot{a}_i u \sin(\psi) + b_i}{\sqrt{(a_i \cos(\psi) - \ddot{a}_i u \sin(\psi) + b_i)^2 + 2\sigma_w^2}} \right] \quad (17)$$

Taking the (17) into account, (14) becomes as

$$BER_{16OQAM}^{rayleigh}(\psi) = \frac{1}{8} \sum_{i=1}^6 w_i [1 - \mathcal{K}(u, \psi, a_i, b_i)] \quad (18)$$

where $\mathcal{K}(\psi, a_i, b_i)$ is defined as

$$\mathcal{K}(\psi, a_i, b_i) = \int_{\mathbb{R}} \frac{e^{-\frac{u^2}{2\sigma_u^2}}}{\sqrt{2\pi\sigma_u^2}} \times \frac{a_i \cos(\psi) - \ddot{a}_i u \sin(\psi) + b_i}{\sqrt{(a_i \cos(\psi) - \ddot{a}_i u \sin(\psi) + b_i)^2 + 2\sigma_w^2}} du \quad (19)$$

by scaling the variable $u_0 = u/\sqrt{2\sigma_u^2}$, the \mathcal{K} integral becomes

$$\mathcal{K}(\psi, a_i, b_i) = \int_{\mathbb{R}} \frac{e^{-u_0^2}}{\sqrt{\pi}} \times \frac{a_i \cos(\psi) - \ddot{a}_i \sqrt{2\sigma_u^2} u_0 \sin(\psi) + b_i}{\sqrt{(a_i \cos(\psi) - \ddot{a}_i \sqrt{2\sigma_u^2} u_0 \sin(\psi) + b_i)^2 + 2\sigma_w^2}} du_0 \quad (20)$$

The \mathcal{K} integral can be accurately approximated by an n -order Gauss-Hermite polynomial expansion as

$$\mathcal{K}(\psi, a_i, b_i) = \frac{1}{\sqrt{\pi}} \sum_{j=1}^n \beta_j f(x_j, \psi, a_i, b_i) \quad (21)$$

where $f(x_j, \psi, a_i, b_i)$ function is defined as

$$f(x_j, \psi, a_i, b_i) = \frac{a_i \cos \psi - \ddot{a}_i \sqrt{2\sigma_u^2} x_j \sin \psi + b_i}{\sqrt{(a_i \cos \psi - \ddot{a}_i \sqrt{2\sigma_u^2} x_j \sin \psi + b_i)^2 + 2\sigma_w^2}} \quad (22)$$

and $\beta_j = (2^{n-1} n! \sqrt{\pi}) / (n^2 [H_{n-1}(x_j)]^2)$, x_j are, respectively, the weights and zeros of the n -order Gauss-Hermite polynomial ($H_n(x) = (-1)^n e^{x^2} \frac{d^n}{dx^n} e^{-x^2}$). The tables containing the values of β_j and x_j can easily be found in literature [10, Table (25.10), p. 924], or can be obtained numerically using numerical computation softwares, such as MATLAB.

It is shown in [26], that using only a number of terms $n = 20$ in (21), provides a very good fitting with the exact results.

By Substituting f in \mathcal{K} and then \mathcal{K} in the BER expression (18), we obtain the final BER expression of 16-OQAM over Rayleigh flat fading channel as given in (23).

$$BER_{16OQAM}^{rayleigh}(\psi) = \frac{1}{8} \sum_{i=1}^6 w_i \left[1 - \frac{1}{\sqrt{\pi}} \sum_{j=1}^n \beta_j \frac{a_i \cos \psi - \ddot{a}_i \sqrt{2\sigma_u^2} x_j \sin \psi + b_i}{\sqrt{(a_i \cos \psi - \ddot{a}_i \sqrt{2\sigma_u^2} x_j \sin \psi + b_i)^2 + 2\sigma_w^2}} \right] \quad (23)$$

3.1. FBMC with Higher Level M-OQAM

For the general case of an M-OQAM constellation, the number of possible classes of bits with different error protection is $\log_2(M)/2$ [27]. In each class the number of bits with different error protection is a multiple of $\sqrt{M}/2$ [28]. Therefore, following a similar derivation as in the 16-OQAM case, the BER of FBMC with higher level M-OQAM will result in more terms in the summation and the final BER expressions for Rayleigh flat fading channel is given by equation (24)

$$BER_{M-OQAM}^{rayleigh}(\psi) = \frac{1}{8} \sum_{i=1}^{\xi} w_i \left[1 - \frac{1}{\sqrt{\pi}} \sum_{j=1}^n \beta_j \frac{a_i \cos \psi - \ddot{a}_i \sqrt{2\sigma_u^2} x_j \sin \psi + b_i}{\sqrt{(a_i \cos \psi - \ddot{a}_i \sqrt{2\sigma_u^2} x_j \sin \psi + b_i)^2 + 2\sigma_w^2}} \right] \quad (24)$$

$$\text{where } \xi = \sum_{l=1}^{\frac{1}{2} \log_2(M)} 2^{l-1} \frac{\sqrt{M}}{2}$$

4. Numerical results

In this section, we present numerical results for the analytical BER expressions that we have derived in the previous section for the considered FBMC-OQAM system. These analytical results, obtained by the Gaussian approximation of the intrinsic-interference, are compared to the ones obtained by simulation where two modulation orders, 16-OQAM and 64-OQAM, are considered. Both analytical and simulation results are given for Rayleigh channel case and different phase rotation shifts.

Figure 3 provides the BER performance of 16-OQAM, Rayleigh flat fading channel and $\psi = 0^\circ, 10^\circ$ and 15° . We clearly observe a degradation of the BER performance when a phase rotation error is occurred. That means that the effect of the intrinsic-interference is harmful even at low SNR. The analytical curves are obtained by using equation (23) and compared to the ones obtained by simulations. We observe from this figure a good agreement between both performance curves which are almost very close. According to these results, we find that the Gaussian intrinsic-interference approximation proved good in the evaluation of FBMC performance in the presence of phase error.

In 64-OQAM modulation and Rayleigh channel case, the BER performance curves are depicted in figure 4 where analytical curves are obtained by using equation (24). Again, we note that the curves obtained by the Gaussian interference approximation for $\psi = 8^\circ$ and 10° have a very good agreement with those obtained by simulation. We recall that the quadrature order of the Gauss-Hermite approximation in equations (23) and (24) was $n = 20$.

This article has been accepted for publication in a future issue of this journal, but has not been fully edited. Content may change prior to final publication in an issue of the journal. To cite the paper please use the doi provided on the Digital Library page.

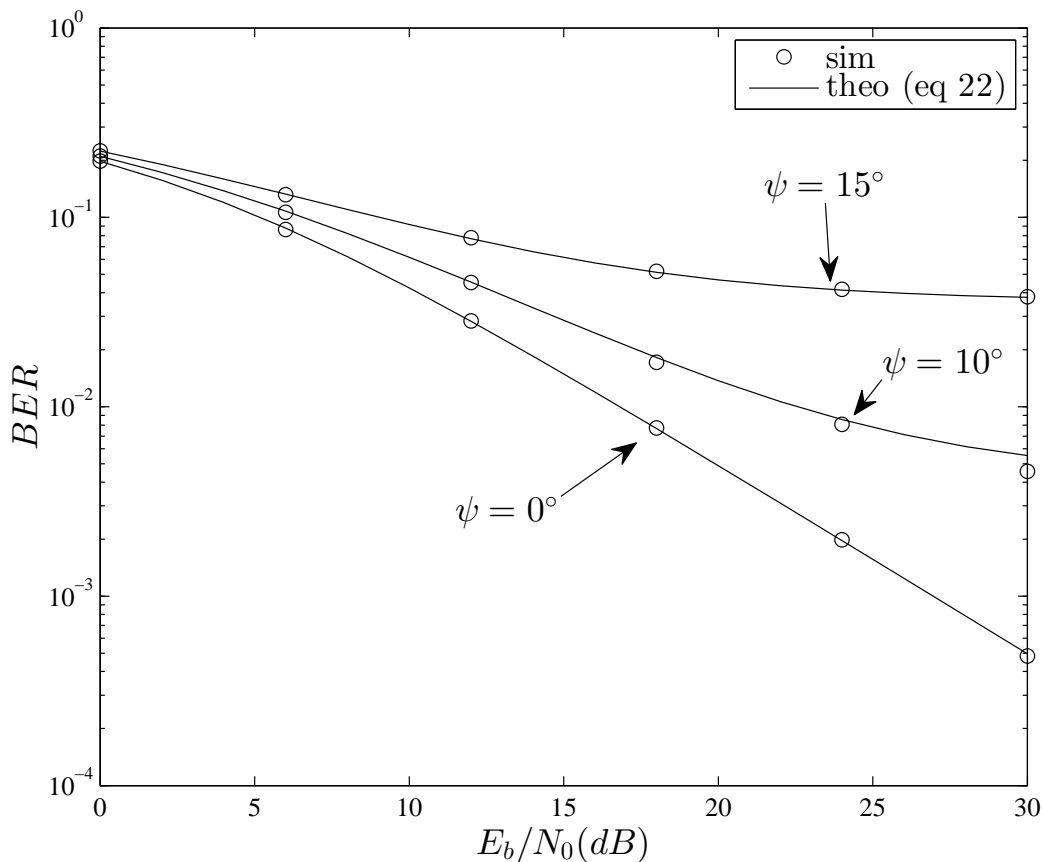


Fig. 3. BER performance for 16-OQAM based FBMC over Rayleigh flat fading channel

5. Conclusion

In this paper, we have provided a general analysis of the BER performance for FBMC-OQAM system in the presence of phase rotation error. We have derived analytical BER expressions for multilevel M-OQAM based FBMC over Rayleigh flat fading channel by approximating the FBMC intrinsic-interference distribution by a Gaussian one. It has been clear that the intrinsic-interference has a significant impact on the BER performance when a phase rotation error is occurred. It is also noticed that the Gaussian interference approximation provide a good accuracy in BER estimation mainly when Rayleigh fading channel is considered. Hence, We have shown that analytical BER curves, obtained by derived expressions in (23), and (24), are almost superposed onto those obtained by simulations.

6. Acknowledgments

This work has been supported by the French ANR-WONG5 project.

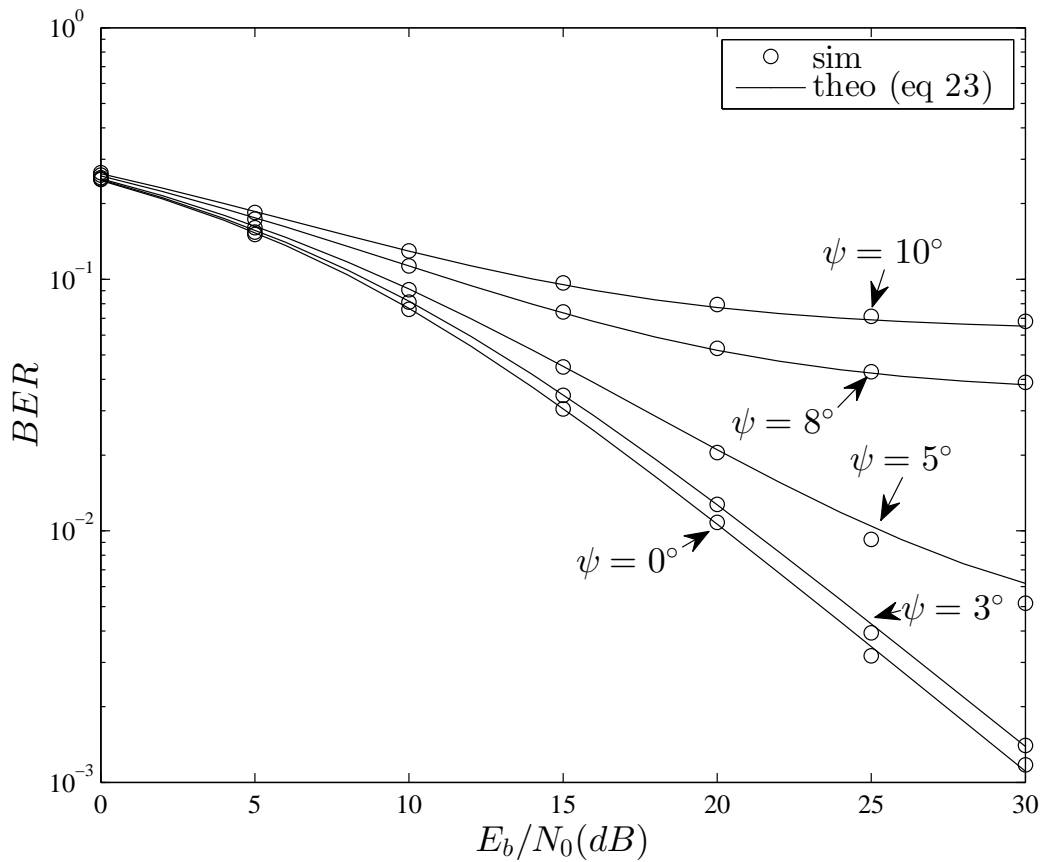


Fig. 4. BER performance for 64-OQAM based FBMC over Rayleigh flat fading channel

7. References

- [1] Farhang-Boroujeny, B., "OFDM versus filter bank multicarrier", *IEEE Signal Process. Mag.*, 28, (3), pp. 92-112, 2011.
- [2] X. Zhang, L. Chen, J. Qiu and J. Abdoli, "On the Waveform for 5G," in *IEEE Communications Magazine*, vol. 54, no. 11, pp. 74-80, November 2016.
- [3] G. Wunder et al, "5GNOW: Non-Orthogonal, asynchronous waveforms for future mobile applications", *IEEE Communications Magazine*, Volume 52, Issue 2, pp. 97-105, February 2014.
- [4] M. Bellanger, "Specification and design of a prototype filter for filter bank based multicarrier transmission", in *Proc. IEEE International Conference Acoustics, Speech, and Signal Processing, Salt Lake City, USA*, pp. 2417-2420, May 2001.
- [5] J. Zhang, M. Zhao, J. Zhong, P. Xiao and T. Yu, "Optimised index modulation for filter bank multicarrier system", in *IET Communications*, vol. 11, no. 4, pp. 459-467, 3 9 2017.
- [6] A. Viholainen, T. Ihalainen, T. H. Stitz, M. Renfors, M. Bellanger, "Prototype filter design for filter bank based multicarrier transmission", *17th European Signal Processing Conference*, 2009.

- [7] H. Hosseini, A. Anpalagan, K. Raahemifar, S. Erkucuk, S. Habib, "Joint wavelet-based spectrum sensing and FBMC modulation for cognitive mmWave small cell networks", *IET Communications*, Volume 10, Issue 14, September 2016, p. 1803 - 1809.
- [8] J. Dou, Z. Zhang, J. Dang, L. Wu, Y. Wei, C. Sun, "Properties and achievable data rate of a cyclic prefix based imperfect reconstruction filter bank multiple access system", *IET Communications*, Volume 10, Issue 17, November 2016, p. 2427 - 2434.
- [9] R. Zakaria and D. Le-Ruyet, "SER analysis by Gaussian interference approximation for filter bank based multicarrier system in the presence of phase error", *IEEE International Conference on Communications (ICC), 2015*.
- [10] H. Bouhadda, H. Shaiek, Y. Medjahdi, D. Roviras, R. Zayani, and R. Bouallegue, "Sensitivity analysis of FBMC signals to non linear phase distortion", *IEEE International Conference on Communications Workshops (ICC), 2014*.
- [11] P. Siohan, C. Siclet, and N. Lacaille, "Analysis and design of OFDM/OQAM systems based on filter bank theory", *IEEE Transaction on Signal Processing*, vol. 50, no. 5, pp. 1170-1183, May 2002.
- [12] R. Zayani, H. Shaiek, D. Roviras and Y. Medjahdi, "Closed-Form BER Expression for (QAM or OQAM)-Based OFDM System With HPA Nonlinearity Over Rayleigh Fading Channel", *IEEE Wireless Communications Letters*, vol. 4, issue 1, pp. 38-41, Feb 2015.
- [13] D. Katselis, E. Kofidis, A. Rontogiannis, S. Theodoridis, "Preamble-based channel estimation for CP-OFDM and OFDM/OQAM systems: A comparative study", *IEEE Trans. Signal Process.*, vol. 58, no. 5, pp. 2911-2916, May 2010.
- [14] C. Li, P. Siohan, R. Legouable, "2dB better than CP-OFDM with OFDM/OQAM for preamble-based channel estimation", *Proc. Int. 675 Conf. Commun.*, pp. 1302-1306, May 2008.
- [15] J. Du, S. Signell, "Novel preamble-based channel estimation for OFDM/OQAM systems", *Proc. IEEE Int. Conf. Commun.*, pp. 14-18, Jun. 2008.
- [16] C. Li, J.-P. Javardin, R. Legouable, A. Skrzypczak, P. Siohan, "Channel estimation methods for preamble-based OFDM/OQAM modulations", *Proc. European Wireless Conf.*, pp. 59-64, Mar. 2007.
- [17] D. Kong, D. Qu, T. Jiang, "Time domain channel estimation for OQAM-OFDM systems: Algorithms and performance bounds", *IEEE Trans. Signal Process.*, vol. 62, no. 2, pp. 322-330, Jan. 2014.
- [18] E. Kofidis, "Short preamble-based estimation of highly frequency selective channels in FBMC/OQAM", *Proc. IEEE Int. Conf. Acoust. Speech Signal Process.*, pp. 8058-8062, May 2014.
- [19] R. Nissel and M. Rupp, "Bit error probability for pilot-symbol aided channel estimation in FBMC-OQAM," *2016 IEEE International Conference on Communications (ICC), Kuala Lumpur*, pp. 1-6, 2016.

- [20] V. Savaux, F. Bader, "Mean square error analysis and linear minimum mean square error application for preamble-based channel estimation in orthogonal frequency division multiplexing/offset quadrature amplitude modulation systems", *IET Commun.*, vol. 9, no. 14, pp. 1763-1773, Aug. 2015.
- [21] S. Hu, Z. Liu, Y. L. Guan, C. Jin, Y. Huang and J. M. Wu, "Training Sequence Design for Efficient Channel Estimation in MIMO-FBMC Systems," in *IEEE Access*, vol. 5, no. , pp. 4747-4758, 2017.
- [22] Mahmoud Aldababseh and Ali Jamoos, Estimation of FBMC/OQAM Fading Channels Using Dual Kalman Filters, *The Scientific World Journal*, vol. 2014, Article ID 586403, 9 pages, 2014.
- [23] E. Kofidis, "Channel estimation in filter bank-based multicarrier systems: Challenges and solutions", *Proc. IEEE 6th Int. Symp. Commun. Control Signal Process.*, pp. 453-456, Mar. 2014.
- [24] X. Tang, M. S. Alouini, and A. J. Goldsmith, "Effect of Channel Estimation Error on M-QAM BER performance in Rayleigh fading", *IEEE Transaction on Communications*, vol. 47, no. 12, Dec. 1999.
- [25] M. K. Simon, "On the bit-error probability of differentially encoded QPSK and offset QPSK in the presence of carrier synchronization," in *IEEE Transactions on Communications*, vol. 54, no. 5, pp. 806-812, May 2006.
- [26] J. F. Paris, M. C. Aguayo-Torres, and J. T. Entrambasaguas, "Impact of Channel Estimation Error on Adaptive Modulation Performance in Flat Fading", *IEEE Transaction on Communications*, vol. 52, no. 5, May 2004.
- [27] N. M. B. Souto, F. A. B. Cercas, R. Dinis and J. C. M. Silva, "On the BER Performance of Hierarchical M-QAM Constellations With Diversity and Imperfect Channel Estimation," in *IEEE Transactions on Communications*, vol. 55, no. 10, pp. 1852-1856, Oct. 2007.
- [28] P. K. Vitthaladevuni and M. S. Alouini, "A recursive algorithm for the exact BER computation of generalized hierarchical QAM constellations," in *IEEE Transactions on Information Theory*, vol. 49, no. 1, pp. 297-307, Jan 2003.